Published by :
http://www.ijert.org

International Journal of Engineering Research & Technology (IJERT)
ISSN: 2278-0181
Vol. 5 Issue 09, September-2016

Unique Analytical Models for Deriving Fundamental Quasi-Mechanistic Design Parameters for Highway and Airport Pavements

John Ngaya Mukabi
R&D/Design Dept.
Kensetsu Kaihatsu Consulting Engineers Ltd.
Nairobi, Kenya

***Abstract*— Characterization of practically all engineering materials adopted in design and construction is based on their intrinsic elastic properties, which are mathematically defined by elastic/resilient/shear moduli, Poisson's ratio and the stresses and strains that are prevalent within the linear elastic recoverable zone. Nevertheless, determination of these parameters of fundamental importance in not only design, but also simulation modelling and structural performance prediction of civil engineering structures, based on laboratory and in-situ mechanical testing, has been and continues to be one of the foremost challenges to Engineers. Furthermore, an even greater challenge is the meticulous quantitative determination of the elastic stress and strain limits which provide the extrapolative platform for subsequent deformation characteristics based on concepts defined within the Kinematic Hardening Soil Yield Surface (KHSYS) context.**

This Study takes advantage of the prodigious advances made in computer science, modelling and the research and methods of laboratory small strain testing to propose TACH-MD universal analytical models that have been predominantly developed on the basis of these advances. The proposed analytical models provide considerable solutions to the aforementioned challenges and are versatile in application with appreciably high degree confidence levels. Case examples of applications of the proposed models for characterization of various types of geomaterials, generation of performance-based value engineering designs, as well as development of special/particular specifications and construction QCA procedures are also introduced. It is also derived that appropriate application of the proposed analytical models can be useful in the generation of highly precise elastic/resilient parameters that can be directly adopted for design, numerical modelling and modules of modelling geotechnical and civil engineering computer software.

Keywords—Analytical models, elastic; quasi-mechanistic design; pavements; stress; strain.

I. INTRODUCTION

A. Limitations of CBR Based Resillient Modulus Models and Design Parameters

Pavement thickness design prior to the 1986 AASHTO Design Guide was, for all practical purposes, based on experience, soil classification, and the plastic response of pavement materials to static load, *e.g.*, Marshall stability for asphalt concrete and CBR for unbound materials. The potential for fatigue cracking of asphalt concrete and the accumulation of permanent deformations in the unbound materials in flexible pavements under essentially elastic deformation conditions were not considered.

Researchers in the 1950s began using repeated load triaxial tests in the laboratory to evaluate the stiffness and other behavior of pavement materials under conditions that more closely simulated quasi-real traffic loadings in the field [1]. Substantial pioneering contributions in this area were made by a number of Researchers in their work on the deformation characteristics and resilient modulus of compacted subgrades [1]. They found significant differences between values generated from these findings and the CBR approach. This conclusion was substantiated by field data obtained by the California Department of Highways that showed the marked difference in pavement deflections occurring under standing and slowly moving wheel loads [1].

B. Limitations of the MEPD Methodlogy

Notwithstanding their limitations and incongruity, the CBR based resilient modulus models based on failure concepts are still popular in application and do dictate the recommended default values provided in practically all of the conventional Design Guidelines including the most recently developed Mechanistic-Empirical Pavement Design (MEPD) Guidelines. However, given the recent developments in computer science leading to advances in the measurement of small strain stiffness using computer-aided automated systems, recently developed sophisticated models depict a certain degree or significant deviation in the resilient/elastic modulus characteristics and specified default values [2].

Since the resilient/elastic modulus is most integral and elactic properties (including Poisson's ratio, elastic and lateral limit strains) are of great significance in the MEPDG, it is increasingly vital that the same be reviewed based on relatively sophisticated and advanced models. The necessity and importance of reviewing some of the default resilient modulus values and resilient properties that are specified in most guidelines as well as the conventional CBR-M_R models is demonstrated in [2] through examples comparing characteristics and values determined from varying models. Limitations associated with the MEPDG mainly emanate from the fact that most models applied in correlating the design parameters are still widely based on CBR concepts,

International Journal of Engineering Research & Technology (IJERT)
ISSN: 2278-0181
Vol. 5 Issue 09, September-2016

C. Limitations of Numerical Modelling

Mathematical and numerical modeling is a fairly established yet vibrant research area in geotechnical engineering. Its advancement has been accelerated in recent years by many emerging computational techniques as well as the increasing availability of computational power. A wide spectrum of approaches, developed on the basis of continuously advancing understanding of soil behavior, have been extended and applied to solve various problems in geotechnical engineering. These methods are increasingly playing important roles not only in achieving better understanding of fundamental behavior of geomaterials and geostructures but also in ensuring the safety and sustainability of large-scale complex geoengineering projects [3].

On the other hand, in the past decennia, the Finite Element Method (FEM) has been increasingly used for the analysis of geotechnical engineering applications. However, as with every other method, the FEM also has its limitations. These limitations are not always recognized by users of finite element software, which can lead to unreliable designs.

Despite the development of easy-to-use finite element programs, it is difficult to create a good model that enables a realistic analysis of the physical processes involved in a real project and which provides a realistic prediction of design quantities (i.e. displacements, stresses, pore pressures, structural forces, bearing capacity, safety factor, drainage capacity, pumping capacity, etc.). This is particularly true for geotechnical applications because the highly non-linear and heterogeneous character of the soil material is difficult to capture in numerical models. When using the finite element method, soil is modelled by means of a constitutive model (stress-strain relationship) which is formulated in a continuum framework. The choice of the constitutive model and the corresponding set of model parameters are the most important issues to consider when creating a finite element model for a geotechnical project. It forms the main limitation in the numerical modelling process, since the model (no matter how complex) will always be a simplification of the real soil behavior with limitations in capturing a number of realistic features of actual geomaterial behavior [3].

D. Performanced-Based Design Approach

Performance-Based Design (PBD) fundamentally entails that, deformation in ground, pavement materials and geo-structures along with the reciprocal structural deformation and stress states, be comprehensively analyzed by adopting appropriate sophisticated analytical methods, particularly for structures with high exposure to seismic action.

The basic prerequisite of the PBD is that the acceptable level of the damage criteria be specified in engineering terms such as displacements, elastic limit stress state and ductility/ strain limit based on the function; as well dynamic loading and/ or seismic response of the structure.

Based on this background therefore, the method employs initial deformation resistance parameters, namely; Resilient/Elastic Modulus, Initial Shear Modulus and Poisson's Ratio defined within the Region of Initial Deformation (RID), Axial Elastic Limit Strain and the Lateral/Radial Elastic Limit Strain parametrically represented:

$$\{M_R/E_0\,,(G_0)_{(Y_I)},\nu_{(Y_I)},[(\varepsilon_a)_{ELS}(Y_I)],and\ [(\varepsilon_{lat.})_{ELS}(Y_I)]\}$$

for all design purposes. Pre-failure deformation is modeled using the Kinematic Hardening Sub-Yield Surface Limits [4]. This method, which incorporates the CMD (Comprehensive Method of Design), fosters comprehensive analyses, rigorous characterization and advanced performance evaluation through the correlation of the principle physical (soil model/index) and mechanical properties of in-situ ground (subgrade, foundation) and geomaterials; to the main design parameters.

The analytical approach also maintains that all parameters employed for design and geomaterials characterization be directly linked to the in-situ test measurements.

This development has been achieved for the quasi-ND (Non-Destructive) mechanical Dynamic Cone Penetration (DCP) and the ND Seismic Surveys as well as the Vertical and Transient Electrical Sounding (VES/TES) geophysical in-situ methods of testing [5].

E. Advantages and Limitations of Proposed Q-M Design Approach

The main advantages of the Quasi-Mechanistic (Q-M) Design approach include, but are not necessarily limited to: i) virtually all parts of the designs can be mechanistically generated with limited empirical reference providing allowance to the Design Engineer to conveniently vary structural, environmental and economic conditions in order to achieve the most optimum PB-VE (Performance Based Value Engineering) balanced design; ii) the basic and intermediate designs can be expeditiously generated from in-situ DCP test results that are analyzed based on analytical models that generate the design parameters directly from in-situ (field) measurements from, for example, the rate of penetration, P_R or Penetration Index (DCPI) in the case of DCP (Dynamic Cone Penetration) tests [6]; this ensures achievement of high precision and confidence levels of the determined design parameters, and enables the Design Engineer to expeditiously deliver the basic/intermediate designs that facilitate speedy decision making and strategic planning of project implementation on the part of Policy and/or Decision Makers; iii) the analysis procedures, model equations and supporting nomographs allow the user to expeditiously obtain counter-check solutions through hand computations; iv) all main model equations are developed with counterpart equations that enable the designer to immediately check and confirm the accuracy of their computations [7]; complex solutions can be obtained from simplified computer programs in the form of worksheets, which facilitates speedy computation [8], [9] and [10]; v) vital engineering parameters necessary in ensuring the achievement of a balanced, economic and PB-VE designs can be computed in "optimal" form from the model equations; vi) modifications, advances and further sophistication can be realized without much complication.

Limitations of the proposed Q-M method are rather similar, although to a lesser extent due to the incorporation of the laboratory and in-situ testing aspects, to the ones mentioned in Section C.

International Journal of Engineering Research & Technology (IJERT)
ISSN: 2278-0181
Vol. 5 Issue 09, September-2016

II. EXPERIMENTAL TESTING

A. Design of Laboratory Testing Regime

1) Main objective: The comprehensive laboratory testing regime was designed with the main objective of acquiring reliable data and information for advancing Research & Innovation for Sustainable Development (RISD) aimed at evolving geo-scientific theories, geomathematical models and geotechnical engineering concepts that would culminate in the development of high precision confidence levels of sophisticated simulation and advanced structural performance prediction models applicable for enhanced Value Engineering Designs and Technologies (VEDs and VETs).

2) Application of appropriate soil mechanics principles: In designing the laboratory testing regime, considerations were made in ensuring appropriate application of the fundamental principles of soil meachanics. In particular, the contribution and influence of the nature, size, and texture of the soil particles, mechanical stability due to inter-particle interaction, particle agglomeration due to cementation and long-term secondary consolidation (creep) on the strength, elastic/resilient and failure characteristics of pavement and subgrade geomaterials.

Essentially, the considerations were made for: i) reconstituted/remolded materials for pavement layers (the actual form in which they are usually used); and, ii) natural materials existing in an "undisturbed" state that have undergone an appreciable amount of secondary consolidation (as would be considered for foundation ground and subgrade).

3) Main conditions of testing considered: The basic conditions of testing considered include, but are not limited to: i) materials storage; ii) geomaterials batching and sample preparation; iiii) conditions of specimen moulding; iv) mode of compaction; v) curing conditions; vi) soaking conditions; vii) mode of consolidation; viii) loading conditions; and, ix) appropriate method of stage and post-shearing deformation measurements.

Four main conditions of molding of test specimens were adopted; namely: i) OBRM batching ratios; ii) OPMC binder ratios; iii) mode of geosynthetics reinforcement; and, iv) multi-layer configuration.

B. Basic Properties of Geomaterials Tested

In this research study, eleven types of geomaterials were tested including: i) expansive black cotton soils from the Lake Basin Region of Kenya and the Jonglei State in Southern Sudan; ii) fine-grained silty clays from the Baraawe Region of Somalia; iii) granular lateritic gravels from Isiolo County in Kenya, Juba City in Southern Sudan and Bujumbura City in Burundi; iv) calcarous gravel from Baraawe Region of Somalia; v) limestone and quartzic gravels from Bossaso City in Puntland State of Somalia; vi) volcanic ash, weathered lateritic gravel, crushed graded rock (stone) aggregates from the Oromo Region of Ethiopia; vii) pozzolanic geomaterial from Songwe in Tanzania; viii) unbound mechanically stabilized at OBR (Optimum Batching Ratio); ix) unbound mechanically stabilized with geosynthetics; x) OPMC (Optimum Mechanical & Chemical) stabilized; and, xi) OPMC-GRI (Geosynthetics Reinforcement/Improvement) geomaterials.

Various modes of batching were employed consisting of a number of the aforementioned geomaterials. Details on the basic properties and characteristics of the geomaterials tested for purposes of developing the proposed analytical models are provided in [11] and [12].

C. Method of Determining Optimum Batching Ratio (OBR)

Since the blending involves mixing proportions of clays, gravels and aggregates, determination of the OBR is basically carried out on the basis of: i) the evaluation of the Plasticity Index (PI) limiting values in relation to the specified design values (refer to graphical example in Fig. 1); and, ii) based on the results from i) and mechanical laboratory tests, generation of quasi-mechanistic characteristic curves upon which the OBR is determined as depicted in Fig. 2.

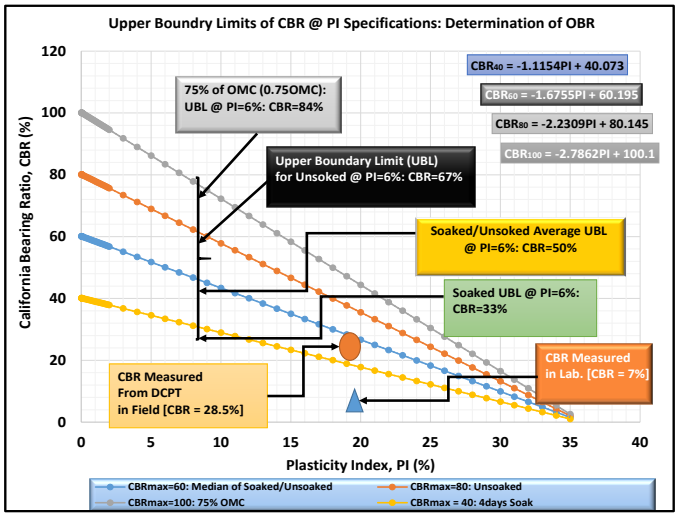

Fig. 1. Example of graphical evaluation of PI limits for determination of OBR.

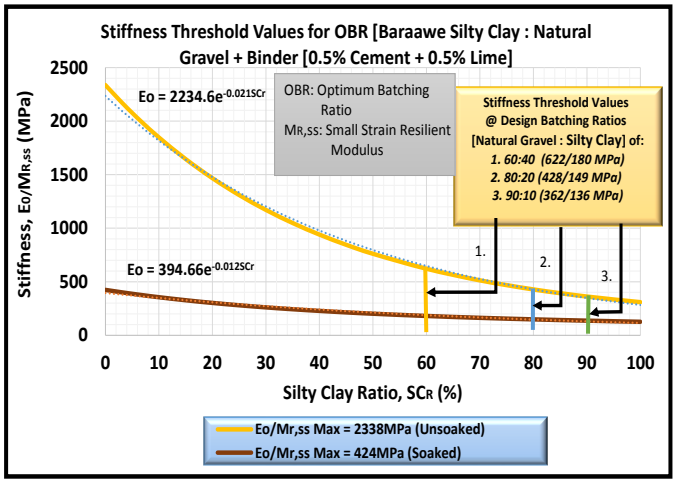

Fig. 2. Determination of OBR based on stiffness and silty clay ratio.

D. Mode of Deformation Measurement

The mode of deformation measurement (vertical/axial and lateral/radial strains) is depicted in Fig. 2. This mode of measurement was espoused for all UCS (Unconfined Compression Strength) and triaxial tests.

International Journal of Engineering Research & Technology (IJERT)
ISSN: 2278-0181
Vol. 5 Issue 09, September-2016

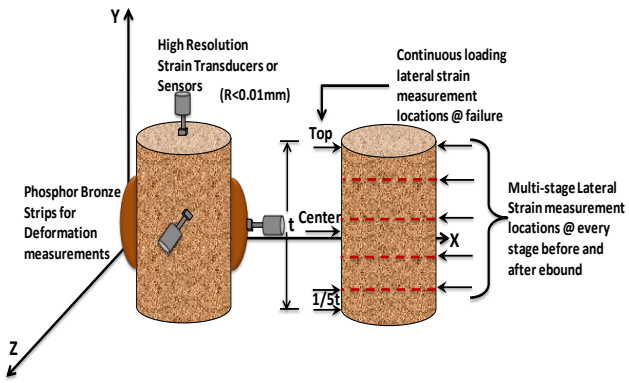

Fig. 3. Mode of deformation measurements for UCS and triaxial tests.

E. Laboratory Testing Protocols

Three modes of loading were adopted under the UCS and triaxial testing protocols to simulate static loads for parked motor vehicles/aircrafts, quasi-dynamic loads for motor vehicles/aircrafts that are taxing and dynamic loads for motor vehicles/aircrafts that are speeding/landing and taking off.

1) Criteria for proposed multi-stage loading: In designing the multi-stage loading test regime, it is important to consider whether or not the highway or airport runway will be subjected to high intensity dynamic loading. In the case of low volume traffic it is then imperative that a more realistic approach to simulate loading that takes into account a rebound effect due to post-dynamic-static loading stress release, is adopted. However, a number of limited tests under sustained dynamic loading to simulate critical state conditions and future expansion considerations should also be undertaken. A graphical example of a multi-stage dynamic → static → dynamic testing protocol is given in Fig. 4.

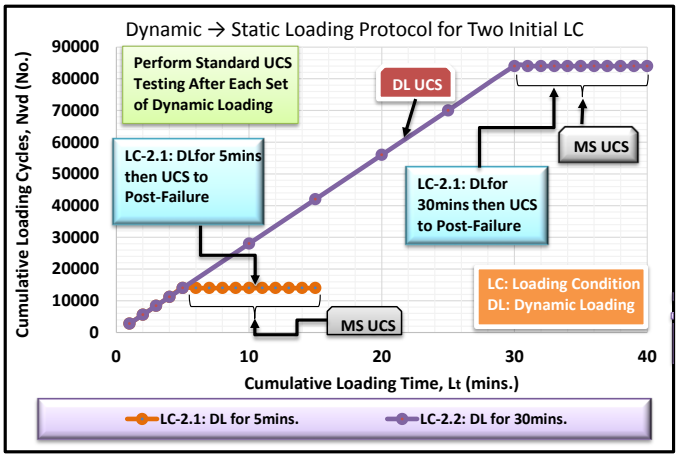

Fig. 4. Example of multi-stage *dynamic* → *static* → *dynamic* protocol

2) Cumulative loading – rebound time protocol: This protocol basically involves multi-stage dynamic loading of the specimens whereby a designated period of rebounding is allowed prior to proceeding to the next stage of reloading as depicted in Fig. 5. During the rebound stage, precise measurements are made of the axial and lateral deformation.

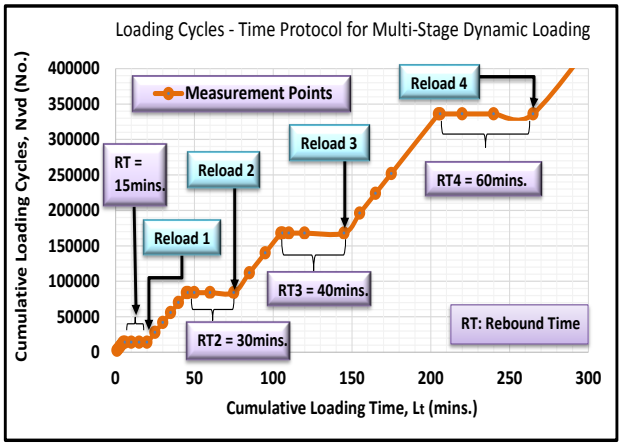

Fig. 5. Cumulative loading – rebound time multi-stage testing protocol.

F. In-situ (Field) Testing Regime

For purposes of design and research, numerous in-situ tests were carried out on existing native subgrades as well as existing and freshly constructed subbase, base course and asphalt concrete pavement layers [7] and [14].

III. Case Example of Materials Characterization

A. Background in Brief

Rigorous testing and comprehensive characterization of various types of geomaterials has been undertaken during the course of this research [11], [12 and [15], the findings of which have been adopted in developing the analytical models introduced in Section IV, PB-VE design guidelines, standard specifications and QCA (Quality Control & Assurance) procedures, which have been widely adopted within the East and Central Africa Region [16] and [17].

B. Progressive Deformation Impacted by Dynamic Loading

An example of a black cotton soil specimen subjected to perpetual vibrational dynamic loading is depicted in Fig. 6. The data was acquired from Feasibility Studies that were conducted under JICA (Japan International Cooperative Agency) Grant Aid for the Western Kenya Rural Roads Improvement Project.

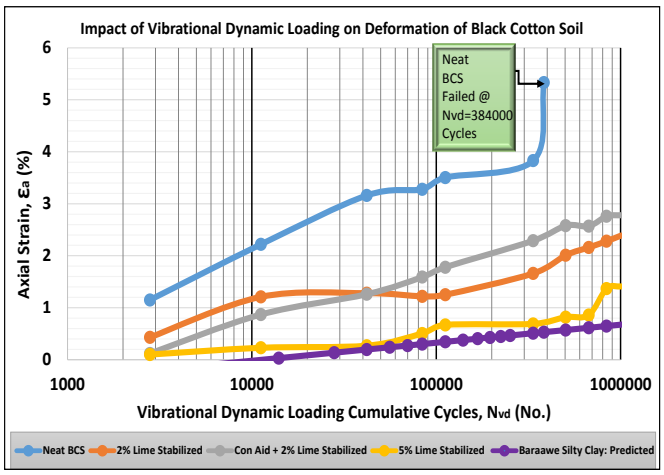

Fig. 6. Impact of vibrational dynamic loading on the deformation properties of problematic black cotton soil from the Lake Basin Region in Kenya

International Journal of Engineering Research & Technology (IJERT)
ISSN: 2278-0181
Vol. 5 Issue 09, September-2016

The black cotton soils were sampled along the Homa Bay - Mbita, Rongo - Ogembo and Bumala – Port Victoria Roads. The variation in the magnitude and rate of deformation of the BCSs as a result of varying modes of stabilization and binder quantities can well be appreciated from this figure.

C. Elastic/Initial Resilient Properties

Elastic/Resilient properties for batched geomaterials to be adopted for the base layer construction of the Baraawe runway pavement, taxiway and aprons in Somalia are depicted in Figs. 7, 8 and 9, for the stiffness, Poisson's ratio, and stiffness summary, respectively. The figures are a representation of nomographs that are to be adopted for Quality and Binder [Cement + Lime] Content Control with respect to the various parameters of the batched Baraawe geomaterials comprising of Baraawe Silty Clay and Calcarous Gravel.

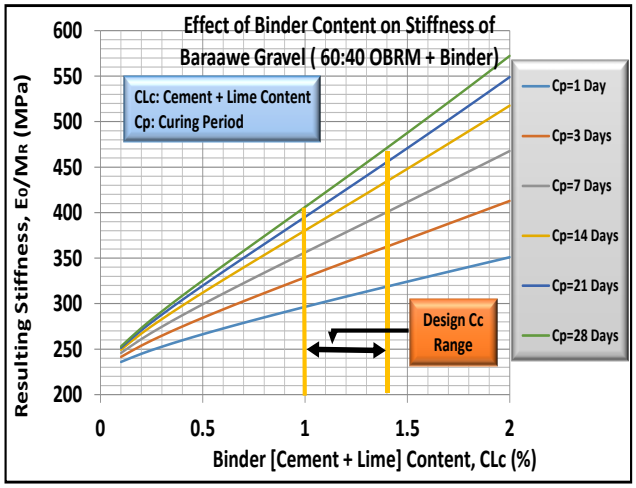

Fig. 7. Nomograph for determining optimum binder content for design, special specifications and QCA for stiffness of the 60:40 [silty clay:gravel] batched geomaterials.

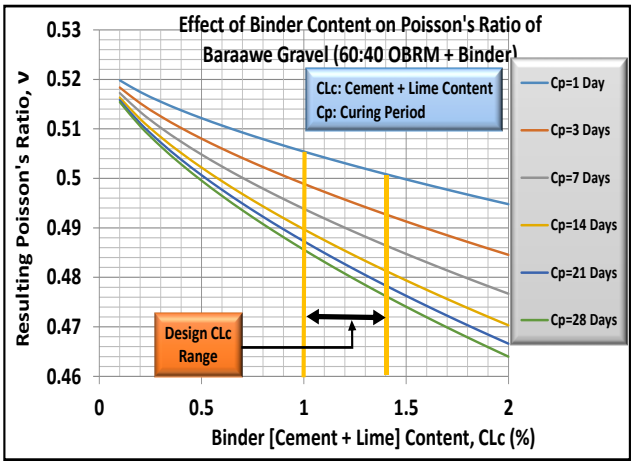

Fig. 8. Nomograph for determining optimum binder content for design, special specifications and QCA for Poisson's ratio of the 60:40 [silty clay:gravel] batched geomaterials

Materials for the priority option design are batched @ ratios of 60:40 [Silty Clay : Gravel], whilst the "Fall Back" options are batched @ ratios of 80:20; 90:10 and 100:0; all of which are bound at different cement + lime ratios. It is essential to note that the Design Binder Content [Cement + Lime] is minimal: within a range of 1 ~ 1.4% by volume for geomaterials batched @ 60:40 and 80:20 and increase to 1.3 ~ 1.7% for the 90:10 and 1.6 ~ 2% for the 100:0% for all the Elastic/Resilient properties [15]. The reciprocal influence of curing and binder content on the initial deformation resistance of batched Baraawe geomaterials can indeed be appreciated.

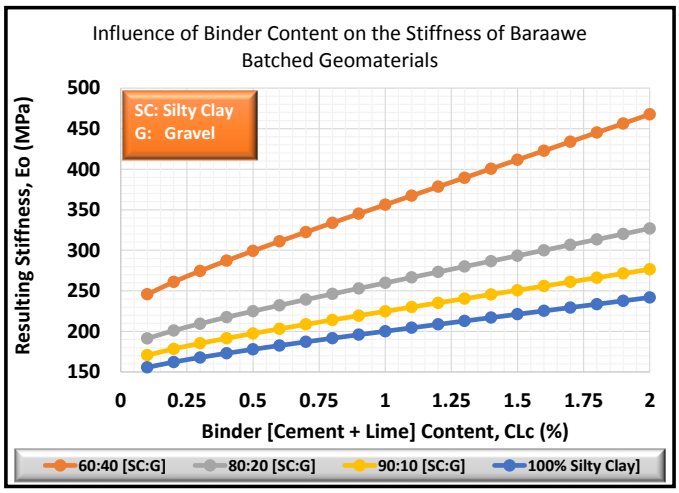

Fig. 9. Summary of the stiffness characteristic curves for the [silty clay:gravel] batched geomaterials @ 7 days cure (particle agglomeration).

D. Performance Simulation

Performance simulation is carried out mainly in consideration of extreme changes in environmental conditions and factors with respect to the limiting design and characteristic parameters of the batched geomaterials to be adopted for the construction of the base layer. Based on the prevailing climatic conditions in the project area, it is imperative that moisture ~ suction variation be analyzed for both suction and dilatant characteristics.

Characteristic simulation is based on TACH-MSV models defined in detail in [18]and [19] for matric suction and moisture increase accordingly.

1) Matric suction effect (decrease in moisture content):

The simulation results for the matric suction (decrease in moisture content) effect for the Baraawe Region in Somalia are presented in Table I, whilst the characteristic curves are graphically plotted in Fig. 10. On the other hand, the simulation results for the dilatancy (increase in moisture content) effect are presented in Table II, whilst the characteristic curves are graphically plotted in Fig. 11. The following salient derivations can be made from the simulation results for the suction effect: i) increase in suction stress causes an exponential increase in the stiffness of all batched geomaterials; in particular, the characteristic increase is more significant for the geomaterial batched @ the ratio of 60:40 containing more of the Baraawe calcarous gravel, a behavior which may be attributed to the sensitivity of gravel geomaterials to effects of confining stresses; ii) at least a 1% suction effect is necessary in order to achieve the required design stiffness for the all the batched base materials; iii) the simulation results indicate that the Ideal Limiting Suction

International Journal of Engineering Research & Technology (IJERT)
ISSN: 2278-0181
Vol. 5 Issue 09, September-2016

Effect (ILSE) should be maintained within 1 and 3%; i.e; $1 \leq ILSE \leq 3\%$. Given the hot and dry climatic conditions that are prevalent in Baraawe for most part of the year, further monitoring during construction in the dry season was recommended. The impact of plasticity index on the magnitude of the matric suction effect can also be well appreciated for all the geomaterials batched at varying ratios.

TABLE I. SUMMARY OF STIFFNESS PARAMETERS SUBJECTED TO MATRIC SUCTION EFFECTS

Effect of Suction (Decrease in Moisture Content) for Batched BC				
Moisture Content, Mc (%)	Resulting Stiffness for 60:40 Batching (MPa)	Resulting Stiffness for 80:20 Batching (MPa)	Resulting Stiffness for 90:10 Batching (MPa)	Resulting Stiffness for 100:0 Batching (MPa)
MRi (Mpa)	180	149	136	126
PI (%)	12	14	15	16
0	151	127	121	111
1	200	169	161	148
2	266	224	214	196
3	353	297	284	261
4	469	395	377	347
5	623	525	501	461

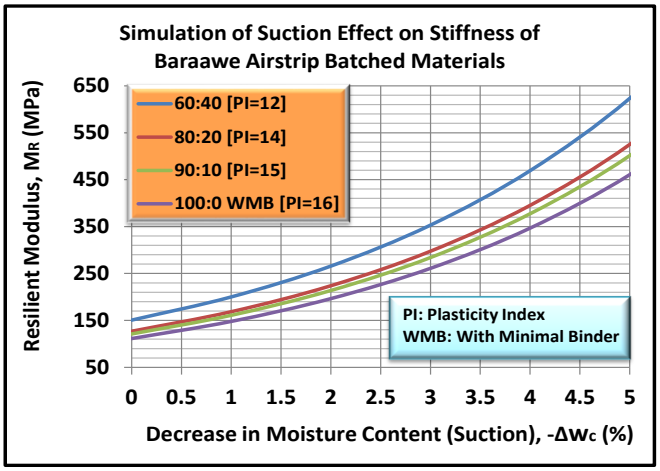

Fig. 10. Graphical representation of the simulation results depicting the matric suction effect on the stiffness of batched geomaterials

2) Dilatancy Effect (Increase in Moisture Content): The simulation results for the dilatancy (increase in moisture content) effect indicate that, for the adopted PI values: i) the limiting value for increase in moisture for the 60:40 batched geomaterial is higher; $M_C = 6.6\%$; ii) the limiting value for increase in moisture for the 80:20 batched geomaterial is moderate; $M_C = 3.9\%$; iii) the limiting value for increase in moisture for the 90:10 batched geomaterial is low; $M_C = 2.5\%$; and, iv) the limiting value for increase in moisture for the 100:0 batched geomaterial is very low; $M_C = 1.3\%$.

These results imply that the geomaterials batched at 90:10 and 100:0 would require additional mitigation measures such as implementation of a secondary shoulder to ensure that the moisture ~ suction variation within the pavement structure is contained to a minimal.

TABLE II. SUMMARY OF STIFFNESS PARAMETERS SUBJECTED TO DILATANCY EFFECTS

Dilatancy Effect (Increase in Moisture Content) for Batched BC				
Moisture Content, Mc (%)	Resulting Stiffness for 60:40 Batching (MPa)	Resulting Stiffness for 80:20 Batching (MPa)	Resulting Stiffness for 90:10 Batching (MPa)	Resulting Stiffness for 100:0 Batching (MPa)
MRi (MPa)	180	149	136	126
PI (%)	12	14	15	16
0	175	144	131	122
1	164	135	123	113
1.3	160	132	120	111
2	153	126	115	106
2.5	148	122	111	102
3	143	118	107	99
3.9	134	111	101	93
5	124	102	93	86
5.4	121	100	91	84
6	116	96	87	81
6.6	111	92	84	77
7	108	89	81	75
8	101	83	76	70
9	95	78	71	66
10	88	73	66	61
12.3	75	62	57	52
14	67	55	50	47

Note: Highlighted Cells indicate the Required Design Values

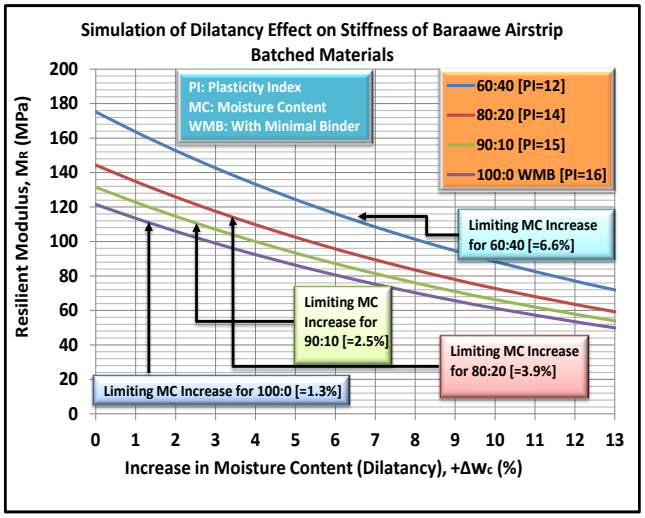

Fig. 11. Graphical representation of the simulation results depicting the moisture content increase effect on the stiffness of batched geomaterials

Detailed analyses and discussions in relation to the impact of moisture ~ suction variation on the small strain elastic/resilient properties of tropical geomaterials subjected to dynamic loading are made in [18] and [19].

E. Specification Considerations Based on Test Results

Based on the laboratory and in-situ (field) test results and analyses carried out for research and design purposes, several aspects considered vital in incorporating in the special/particular specifications were derived.

International Journal of Engineering Research & Technology (IJERT)
ISSN: 2278-0181
Vol. 5 Issue 09, September-2016

The main aspects of concern include, but are not necessarily limited to: i) determination of appropriate binder content and agglomeration (curing) period for strength and stiffness specifications; ii) structural and filter layer specifications; iii) determination of limit values (Table III).

TABLE III. SUMMARY OF LIMITING ELASTIC PROPERTIES

S/N	Type of Batched Geomaterial	QCA Parameter	Values for Varying Soaking Conditions		
			4 Days Soak	Partially Soaked	Unsoaked
1.	60:40 Batching [Silty Clay : Gravel] + Binder [0.5% Cement + 0.5% Lime]	Elastic/Resilient Modulus (MPa)	≥ 160	180 ~ 580	≥ 600
2.		Poisson's Ratio	≤ 0.55	0.53 ~ 0.48	≤ 0.46
3.	80:20 Batching [Silty Clay : Gravel] + Binder [0.5% Cement + 0.5% Lime]	Elastic/Resilient Modulus (MPa)	≥ 120	140 ~3 80	≥ 400
4.		Poisson's Ratio	≤ 0.57	0.55 ~ 0.47	≤ 0.49
5.	90:10 Batching [Silty Clay : Gravel] + Binder [0.5% Cement + 0.5% Lime]	Elastic/Resilient Modulus (MPa)	≥ 100	120 ~ 330	≥ 350
6.		Poisson's Ratio	≤ 0.59	0.57 ~ 0.49	≤ 0.51
7.	100:0 Batching [Silty Clay : Gravel] + Binder [0.5% Cement + 0.5% Lime]	Elastic/Resilient Modulus (MPa)	≥ 90	100 ~ 280	≥ 300
8.		Poisson's Ratio	≤ 0.6	0.58 ~ 0.5	≤ 0.52

F. Analysis of In-situ Test Results

Detailed analysis and the findings from in-situ (field) tests performed within the framework of this elaborate study are reported in [14].

IV. TACH ANALYTICAL MODELS DEVELOPED & PROPOSED

The proposed TACH-MD analytical models are developed on the basis of geoscientific and geomathematical theories considering pragmatic engineering concepts and applications. The data adopted in its development covers a wide range of materials from very soft clays, stiff to hard clayey geomaterials, sands, silts, hydraulic and asphaltic bound materials, concrete and rocks [20].

The very basic procedure of developing the models involved: i) collection of universal data from small strain laboratory testing; ii) collection of universal data from field (in-situ) geophysical testing; iii) development of correlating equations; iv) application of equations to correlate and generate relevant characteristic curves; v) application of the TACH-MD universal iterative/regression concept to develop universal model equations; vi) application of CSSR (Consolidation Shear Stress Ratio) concepts for probing changes, and magnitudes thereof, in states of stress and strain during consolidation in relation to the original state of stress and stress paths perturbed [4]; vii) comprehensive study of the relevant and most pragmatically applicable constitutive and numerical models; and, vii) application of optimization mathematical concepts to simplify models. In the development of the proposed models, various influencing factors were considered including, but not limited to, type and nature of geomaterials, voids ratio, porosity, density, clay content, confining stress, moisture ~ suction variation, mechanical stabilization, chemical stabilization, binder type, and temperature (thermal effects) particularly for asphaltic bound materials and concrete.

The importance of characterization of small strain properties in geotechnical engineering can very well be appreciated from Figs. 12 and 13. Whereas Fig. 12 clearly demonstrates the fact that, under normal circumstances, most civil engineering structures undergo deformation within the small strain region, both Figs. 12 and 13 clearly show that geomaterials exhibit very small linear elastic and recoverable elastic strain limits. As a consequence, it is imperative that concentration on proper interpretation and deep understanding of a wide range of geomaterials characteristics within this zone be invested.

This fact led to the extensive long-term research that culminated in the development of the analytical models proposed in the subsequent sections.

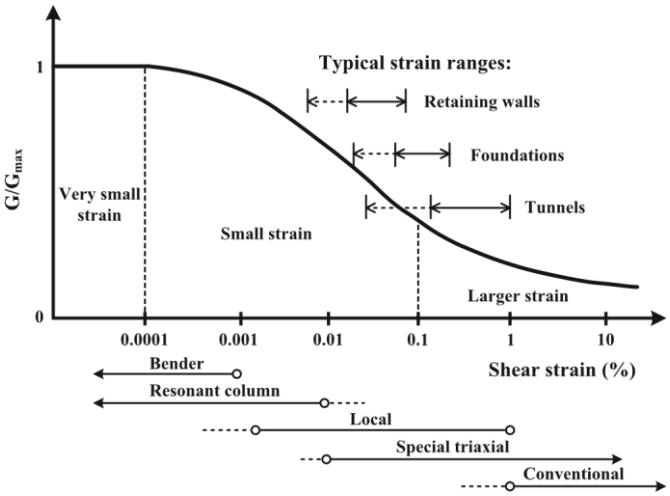

Fig. 12. Example of range of strains for various civil engineering structures under normal working loads and the stiffness decay characteric curve as influenced by the strain level.

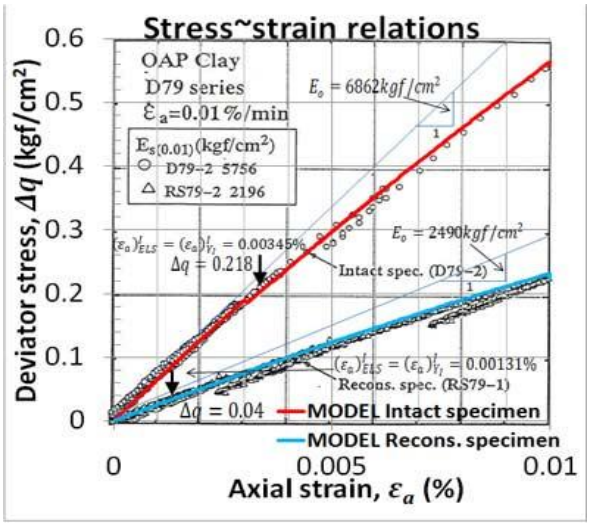

Fig. 13. Example of range of elastic stress and strain limits.

International Journal of Engineering Research & Technology (IJERT)
ISSN: 2278-0181
Vol. 5 Issue 09, September-2016

A. Models for Deriving Elastic Modulus

1) Determination at varying states of stress:

a) Fundamental necessity for development of models: Changes consistently occur in the states of stress of foundation ground mainly as a result of external forces such as imposed loads and moisture ~ suction variations emanating from environmental conditions and factors. On the other hand, almost all construction materials utilized for civil engineering purposes are extruded, reconstituted (remolded) and subsequently factory and/or in-situ processed through compaction and/or re-consolidation thereby causing insurmountable changes in the inherent structure and properties of the materials. This cerainly impacts strongly on the magnitudes of the design parameters and the post-construction material characteristics. Various methods of sampling and laboratory testing have been developed in an effort to replicate the original conditions. Although noticeable advances have been made in this regard, it has proven impossible to achieve ideal replication. The development of models that can retrace the original stress-strain-time histories is therefore an imperative.

An appreciably versatile quasi-mechanistic geo-mathematical model for examining such changes (TACH-GECPROM), is introduced [4]. GECPROM is designed to probe and estimate changes in vital geo-properties for clayey geomaterials and ground. The significant advantage of this model is that; various geotechnical changes and geo-structural behavior can be modeled from a single sophisticated experimental test, whilst simultaneously catering for the effects of drainage conditions, loading rate, and consolidation stress-strain-time history.

The fundamental model equation for the elastic modulus mainly developed from CSSR concepts and elastic theory, which defines the progressive changes in stiffness with corresponding changes in the states of stress for any given consolidation-stress-strain-time history (CSSTH), is expressed as (1) and (2).

$$[E_o]_{p'} = \left\{ \mathcal{A}_{p'_o} \left[(K_{cs})^{\alpha} \times \left(\frac{p'}{p'_o} \right)^{\beta} \right] + \mathcal{B}_{p'_o}^{K_{cs}} \right\} \times [E_o]_{p'_o} \quad (1)$$

$$[E_o]_{\sigma a0'} = \left\{ \mathcal{A}_{\sigma a0'_o} \left[(K_{cs})^{\alpha} \times \left(\frac{\sigma a0'}{\sigma a0'_o} \right)^{\beta} \right] + \mathcal{B}_{\sigma a0'_o}^{K_{cs}} \right\} \times [E_o]_{\sigma a0'_o} \quad (2)$$

where $[E_o]_{p'}$ is the initial elastic modulus at a variable stress point p', $K_{cs}=\sigma'_r/\sigma'_a$ is the arbitrary or designated consolidation stress ratio traced to p', $[E_o]_{p'_o}$ is the initial elastic modulus determined at in-situ overburden pressure, $\mathcal{A}_{p'_o}$=0.86 and $\mathcal{B}_{p'_o}$=0.35 are geomaterial constants, the values of which are applicable for most natural stiff to hard clayey geomaterials, while β=1.16 and α=0.4 for stress states in the 1st quadrant and α=-1 for stress states in the 4th quadrant accordingly determined in the p'~ q stress plane.

b) Applicability: The model is characteristic over a wide range of applications including: i) retracing CSSH to provide data on the range of property and parametric changes that have occurred between the original and reconstituted states of clayey ground and geomaterials; ii) computation of the elastic modulus (stiffness) at any given "current" state of stress; iii) derivation of likely states of deformation; iv) derivation of likely kinematic hardening characteristics, among other applications. Refer to Figs. 15 and 16 for the applied demonstration in geomaterials characterization.

2) Determination at varying overconsolidation ratios

Practially all geomaterials adopted for civil engineering purposes are reconstituted subsequent to which they are remolded through compaction and/or reconsolidation. Essentially therefore, destructuration of the original structure of natural geomaterials always occurs. In this Study, critical destructuration caused by heavy over-densification is simulated by adopting the SHANSEP concept whereby the specimen is reconsolidated well beyond its field overburden stress, σ'_{a0}. It is appreciated that densification within the natural boundary limits of a geomaterial enhances its properties. However, the findings from this study confirm that excessive densification beyond the in-situ yield stress leads to large scale straining (softening) and destruction of cementation, bonding and thixotropic components as well as causing change in the preferred particle orientation and inherent/induced anisotropic properties of natural clayey geomaterials. This characteristic can be modelled using (3) and (4).

$$E_0^R = (E_0)_y^P \times OCR^{-0.39} \quad (3)$$

where, E_0^R is the resulting initial modulus and $(E_0)_y^P$ is the pseudo-yield initial modulus determined at the stress level (pseudo-yield stress) which is higher than the yield stress $(\sigma'_a)_y^P$ and from which the specimen is rebound, defined as;

$$(E_0)_y^P = (E_0)_{@\sigma'_{a0}} \times \left\{ (\sigma'_a)_y^P / (\sigma'_{a0})_y^{NC} \right\}^{0.39} \quad (4)$$

3) Undrained conditions: Refer to (5)and (6).

a) As a classic function: In this case the elastic modulus is determined from the elastic limit stresses and strains $[\Delta\sigma_{dpd,Y_I}$ and $(\varepsilon_a)_{pd,Y_I}]$ defined within the initial yield surface, Y_I; whereby the two parameters are determined from the analytical model equations proposed in [19].

$$E_{0,u,Y_I} = \frac{\Delta\sigma_{du,Y_I}}{(\varepsilon_a)_{u,Y_I}} \quad (5)$$

b) As a function of ELS and mean effective stress:

$$E_{0,Y_I}^u = exp\left\{ 2.381 ln\left(9678.668 p_o'^{-0.58} \left[(\varepsilon_a)_{u,Y_I} \right]_{ELS}^u \right) \right\} \quad (6)$$

International Journal of Engineering Research & Technology (IJERT)
ISSN: 2278-0181
Vol. 5 Issue 09, September-2016

4) Partially Drained: Refer to (7)and (8).

a) As a classic function:

$$E_{0,pd,Y_I} = \frac{\Delta\sigma_{dpd_{,,}Y_I}}{(\varepsilon_a)_{pd,Y_I}} \quad (7)$$

b) As a function of ELS and mean effective stress:

$$E_{0,Y_I}^{pd} = exp\left\{2.381ln\left(10{,}000p_o'^{-0.58}\left[(\varepsilon_a)_{pd,Y_I}\right]_{ELS}^{pd}\right)\right\} \quad (8)$$

5) Drained conditions: Refer to (9)and (10).

a) As a classic function:

$$E_{0,d,Y_I} = \frac{\Delta\sigma_{dd_{,,}Y_I}}{(\varepsilon_a)_{d,Y_I}} \quad (9)$$

b) As a function of ELS and mean effective stress:

$$E_{0,Y_I}^{d} = exp\left\{2.381ln\left(9678.668p_o'^{-0.602}\left[(\varepsilon_a)_{d,Y_I}\right]_{ELS}^{a}\right)\right\} \quad (10)$$

B. Models for Deriving Shear Modulus

Refer to 1) a) for similar narrative.

1) Determination at varying states of stress: Employing the TACH-PR Model that correlates elastic modulus to Poisson's ratio defined in (16), the shear modulus is then computed from (11).

$$[G_o]_{p'} = \frac{[E_o]_{p'}}{2\{1.864 - 0.064ln([E_o]_{p'})\}} \quad (11)$$

2) Determination at varying overconsolidation ratios:

$$G_0 = \{(G_0)_{oss}/G_R \times OCR^{-0.39}\} \times (G_0)_{oss} \quad (12)$$

where $(G_0)_{oss}$ is the initial modulus at the designated stress point and $G_R = 290MPa$ is the reference initial shear modulus as determined in this study.

3) Undrained conditions: Refer to (13)

$$[G_o]_u = \frac{exp\left\{2.381ln\left(9678.668p_o'^{-0.58}\left[(\varepsilon_a)_{u,Y_I}\right]_{ELS}^{u}\right)\right\}}{2\{1.864 - 0.064ln([E_o]_u)\}} \quad (13)$$

4) Partially drained conditions: Refer to (14).

$$[G_o]_{pd} = \frac{E_{0,Y_I}^{pd} = exp\left\{2.381ln\left(10{,}000p_o'^{-0.58}\left[(\varepsilon_a)_{pd,Y_I}\right]_{ELS}^{pd}\right)\right\}}{2\{1.864 - 0.064ln([E_o]_{pd})\}} \quad (14)$$

5) Drained conditions: Refer to (15).

$$[G_o]_d = \frac{exp\left\{2.381ln\left(9678.668p_o'^{-0.602}\left[(\varepsilon_a)_{d,Y_I}\right]_{ELS}^{a}\right)\right\}}{2\{1.864 - 0.064ln([E_o]_d)\}} \quad (15)$$

C. Models for Deriving Poisson's Ratio

The elastic modulus and Poisson's ratio are the two most fundamental and principle parameters required in material science and the design of civil engineering structures. Nevertheless, measurement/physical modelling of the Poisson's ratio, the advances in small strain measurements notwithstanding, in consideration of varying drainage conditions, has always posed challenges. This has led to the assumption and/or generalized estimation of Poisson's ratio values in design, performance simulation, modelling, structural performance prediction and evaluation. On the other hand, geomathetical models used in determining crucially important analysis, design and modelling parameters from some of the most popular in-situ methods of testing such as geophysical (near surface wave measurements), Plate Loading (PL) and Falling Weight Deflectometers (FWDs) involve the direct use of the Poisson's ratio.

Given the importance of this parameter and its influence on some of the most vital design parameters including the shear modulus, this study concentrated on developing a straight forward model that is versatile in its application for civil engineering purposes and correlates extremely well with other crucial measurement and design parameters. The model, which was developed on the basis of geoscientific and geomathematical theories considering pragmatic engineering concepts and applications, is validated through comparative analysis with some of the typical values determined from advanced methods of measurement of elastic/dynamic properties. Comparison with typical values that are recommended for use with different civil engineering materials is made and the due corrective measures recommended accordingly. The proposed TACH-PR model that correlates elastic modulus to Poisson's ratio as defined in (16) ~ (22) for varying drainage conditions, can be useful in practically all cases of civil engineering applications [21].

1) Undrained conditions: Refer to (16) ~ (19).

$$[\nu]_{up'} = 0.864 - 0.063ln([E_o]_{up'}) \quad (16)$$

2) Partially drained conditions: Refer to (16).

a) In correlation with undrained elastic modulus:

$$\nu_{pd} = \left\{\frac{[0.6138(E_o)_u + 144.06]}{(E_o)_u}(1.864 - 0.063ln([E_o]_u))\right\} - 1 \quad (17)$$

b) In correlation with drained and undrained moduli ratio:

$$\nu_{pd} = \left\{\frac{(E_o)_d}{(E_o)_u}(1 + \nu_u)\right\} - \frac{(E_o)_d}{(E_o)_u} \quad (18)$$

c) In correlation with undrained moduli ratio:

$$\nu_{pd} = \left\{\frac{0.6469(E_o)_u^{1.03/9}}{(E_o)_u}[1 + (0.864 - 0.063ln([E_o]_{p'}))]\right\} - \frac{0.6469(E_o)_u^{1.03/9}}{(E_o)_u} \quad (19)$$

International Journal of Engineering Research & Technology (IJERT)
ISSN: 2278-0181
Vol. 5 Issue 09, September-2016

3) Drained conditions: Refer to (20) ~ (22).

a) In correlation with undrained elastic modulus:

$$\nu_d = 0.055ln\left((0.864 - 0.063ln([E_o]_{p'})\right) + 0.2477 \quad (20)$$

b) In correlation with drained and undrained moduli ratio:

$$\nu_d = \left\{\frac{(E_o)_d}{(E_o)_u}(1+\nu_u)\right\} - 1 \quad (21)$$

c) In correlation with undrained moduli ratio:

$$\nu_d = \left\{\frac{\left[0.6469(E_o)_u^{1.0379}\right]}{(E_o)_u}\left(1.864 - 0.063ln([E_o]_u)\right)\right\} - 1 \quad (22)$$

D. Model for Determining Elastic Limit Strain (ELS) Threshold

The ELS basically defines the range within which the constitutive behavior of any engineering material is linear elastic and fully recoverable upon *loading → unloading → reloading*. It indeed is one of the most vital parameters in science and engineering theory and practice. Given geomaterials predominantly non-linear behavior from a region of extremely small strains, determination of their precise ELS threshold continues to pose major challenges to researchers and engineers alike. The proposed analytical model in (23) provides means to alleviate this problem. In this case, the factored in-situ elastic modulus measured from the field and/or estimated from UCS tests is adopted in determining the ELS threshold for purposes of developing particular specifications for elastic stress – strain limits and deriving permanent deformation characteristics based on the KHSSS models [4].

1) Determination of ELS at Varying States of Stress

On the other hand, the basic model equation defining the impact of stress states on the elastic limit strain that defines the initial yield surface is expressed as:

$$[\varepsilon_a]_{Y_I}^{\sigma_{ss}} = \frac{\left\{\mathcal{A}_{p_o'}^{\varepsilon}\left[(K_{cs})^l \times \left(\frac{p'}{p_o'}\right)^m\right] + \mathcal{B}_{p_o',\varepsilon}^{K_{cs}}\right\}^{\alpha}}{\psi_{(\varepsilon_a)_{Y_I}}} \times [(\varepsilon_a)_{Y_I}]_{p_o'} \Big|_{\psi_{(\varepsilon_a)_{Y_I}} > 1, \alpha = -1}^{\leq 1, \alpha = +1} \quad (23)$$

where, constants $\mathcal{A}_{p_o'}^{\varepsilon}$=0.98, $\mathcal{B}_{p_o',\varepsilon}$=0.32, l=0.4, for stress states in the 1st quadrant and, l=-1, in the 4th quadrant of the p' ~ q stress plane, while m=1.16.

Note that the multiplier $(\varepsilon_a)_{Y_I}$ on the RHS can be derived from the following [(24) ~ (32)] model equations for OCR, undrained, partially drained and drained conditions.

2) Determination at varying overconsolidation ratios

a) Destructuration: Deterioration leading to the reduction of the initial yield strain $\{(\varepsilon_a)_{ELS}(Y_I)\}$ is modelled based on (24).

$$[\varepsilon_a]_{Y_I}^{R} = (\varepsilon_a)_{Y_I}^{NC} - \mathcal{A}_{ys} \ln OCR \quad (24)$$

where, $[\varepsilon_a]_{Y_I}^{R}$ is the resulting size of the initial yield strain, $(\varepsilon_a)_{Y_I}^{py}$ is the initial yield strain determined at the pseudo-yield stress level and $1 \times 10^{-3} \leq \mathcal{A}_{ys} \leq 3 \times 10^{-3}$ is a constant that is dependent on the stiffness and nature of the geomaterial.

b) Partial restructuration: The model equation for partially restructured ELS achieved through LTC (Long Term Consolidation) of overconsolidated foundation ground and/or geomaterials is defined in (25).

$$[\varepsilon_a]_{Y_I}^{OCR} = 0.0031ln(OCR) + 0.0009 \quad (25)$$

3) Undrained conditions: Refer to (26).

$$(\varepsilon_a)_{u,Y_I} = 0.00010332 \times \left(\frac{E_{0,u,Y_I}}{p_o'}\right)^{-0.58} \times E_{0,u,Y_I} \quad (26)$$

4) Partially drained conditions: Refer to (27) and (28).

a) In Correlation with elastic modulus:

$$(\varepsilon_a)_{pd,Y_I} = 0.000099982 \times \left(\frac{E_{0,pd,Y_I}}{p_o'}\right)^{-0.58} \times E_{0,pd,Y_I} \quad (27)$$

b) In correlation with undrained ELS:

$$(\varepsilon_a)_{pd,Y_I} = \frac{(1+\nu_{pd})}{(1+\nu_u)}(\varepsilon_a)_{u,Y_I} \quad (28)$$

5) Drained conditions: Refer to (29) ~ (32).

a) In Correlation with elastic modulus:

$$(\varepsilon_a)_{d,Y_I} = 0.00013642 \times \left(\frac{E_{0,d,Y_I}}{p_o'}\right)^{-0.602} \times E_{0,d,Y_I} \quad (29)$$

and,

$$(\varepsilon_a)_{d,Y_I} = 8.825 \times 10^{-5} \times \left(\frac{0.6469(E_o)_u^{1.0379}}{p_o'}\right)^{-0.602} \times (E_o)_u^{1.0379} \quad (30)$$

b) In correlation with undrained ELS:

$$(\varepsilon_a)_{d,Y_I} = \frac{(1+\nu_d)}{(1+\nu_u)}(\varepsilon_a)_{u,Y_I} \quad (31)$$

also,

$$[\varepsilon_a]_{d,Y_I}' = 0.8563[\varepsilon_a]_{u,Y_I}^{0.963} \quad (32)$$

E. Model for Determining Elastic Limit Deviator Stress (ELSt) Threshold

In conjunction with the ELS defined in Section D, the ELSt has largely been estimated without any geoscientific basis of determination proposed hitherto. The proposed model

International Journal of Engineering Research & Technology (IJERT)
ISSN: 2278-0181
Vol. 5 Issue 09, September-2016

for defining the elastic limit threshold for the deviator stress is in juxtaposition with the one for the elastic limit strain. Model equations for deriving this vital parameter are provided in (33), (35) and (36) for undrained, partially drained and drained, respectively. The particular specification limits can be determined as per the discussions posed in Section D for determination of the elastic limit strain threshold.

1) Undrained conditions: Refer to (33).

$$[\Delta\sigma_{d,u}]_{ELS} = 0.000095602 \times \left(\frac{E_{0,u,Y_I}}{p_o'}\right)^{-0.58} \times E_{0,u,Y_I}^{\alpha_u} \quad (33)$$

where,

$$\alpha_u = 3.399 \times 10^{-9} \times \left(\frac{E_{0,u,Y_I}}{p_o'}\right)^2 - 8 \times 10^{-6}\left(\frac{E_{0,u,Y_I}}{p_o'}\right) + 2.0046 \quad (34)$$

Note that; $\alpha_u = \alpha_{pd} = \alpha_d$ for undrained, partially drained and drained, respectively.

2) Partially drained conditions: Refer to (35).

$$[\Delta\sigma_{d,pd}]_{ELS} = 0.000095602 \times \left(\frac{E_{0,pd,Y_I}}{p_o'}\right)^{-0.58} \times E_{0,pd,Y_I}^{\alpha_{pd}} \quad (35)$$

3) Drained conditions: Refer to (36).

$$[\Delta\sigma_{d,d}]_{ELS} = 0.0001352 \times \left(\frac{E_{0,d,Y_I}}{p_o'}\right)^{-0.615} \times E_{0,d,Y_I}^{\alpha_d} \quad (36)$$

F. Models for Determining Secondary Stress-Strain Yield Surfaces

The models for determining secondary stress-strain yield surfaces are discussed in [4].

G. Progressive Deformation Model

The importance of developing reliable models for characterizing the progressive deformation of foundation ground and pavement structures subjected to dynamic loading cannot be overemphasized. The proposed models can be applied in determining, more precisely, the characteristics and upper boundary limits within which permanent deformation should be specified (refer to Fig. 14).

$$\varepsilon_a = [0.0279exp(0.0937PI)] \times ln(N_{vdA}) - 0.5045exp(0.057PI) \quad (37a)$$

$$\varepsilon_a = \{0.0279exp(\langle 1.6658 \times 10^{-5}E_0^2 - 0.0155E_0 + 3.53493 \rangle)\} \times ln(N_{vdA}) - 0.5045exp\{\langle 4.43346 \times 10^{-5}E_0^2 - 9.4278 \times 10^{-3}E_0 + 2.50382 \rangle\} \quad (37b)$$

The lateral deformation can be determined based on the model equations defined in (37a) and (37b) by multiplying the RHS with the Poisson's ratio, ν based on the relation: $\varepsilon_{lat.} = \nu\varepsilon_a$ whereby ν is determined from (16) ~ (22).

H. Model for Correlating Elastic and Resilient Moduli

The model for correlating elastic and resilient moduli accounting for the effects of confining stress is developed based on the concepts of KHSSS (Kinematic Hardening Small Strain Stiffness) and resilient moduli determined in accordance with the Long Term Pavement Performance (LTPP) Protocol P46, a standard protocol set forth for M_R testing in 1996, by the US Federal Highway Administration (FHWA). The model equations are defined in (38) and (39).

$$E_0 = (2.4155\sigma_c'^{-0.16})M_R + 0.4367\sigma_c' + 0.8511 \quad (38)$$

$$M_R = \frac{E_0 - (0.4367)\sigma_c' + 0.8511}{2.4155\sigma_c'^{-0.16}} \quad (39)$$

I. Linked Modules

1) Influence of confining stress on elastic/small strain resilient modulus:

$$M_R = \{M_{R,ss}exp(0.0233\sigma_c')\}\sigma_d'^{-[0.0028\sigma_c' + 0.4053]} \quad (40)$$

2) Influence of confining stress on Poisson's rato:

$$[\nu]_u = \{\langle 0.864 - 0.063ln\left([M_{R,ss}]_u\right)\rangle exp(0.0233\sigma_c')\}\sigma_d'^{-[0.0028\sigma_c' + 0.4053]} \quad (41)$$

3) Influence of confining stress on shear modulus:

$$G_0 = \left\{\frac{[E_o]_{p'}}{2\{1.864 - 0.064ln([E_o]_{p'})\}}exp(0.0233\sigma_c')\right\}\sigma_d'^{-[0.0028\sigma_c' + 0.4053]} \quad (42)$$

4) Influence of confining stress on elastic limit strain:

$$(\varepsilon_a)_{d,Y_I} = \left\{\left[0.0001364 \times \left(\frac{E_{0,d,Y_I}}{p_o'}\right)^{-0.602} \times E_{0,d,Y_I}\right]exp(0.0233\sigma_c')\right\}\sigma_d'^{-[0.0028\sigma_c' + 0.4053]} \quad (43)$$

5) Long-term consolidation effects on elastic modulus:

The effect of secondary consolidation on the elastic modulus is known to be minimal within the linear elastic and recoverable zone for "intact" specimens. This effect can be quantified by applying (44) for the intact and (45) for the reconstituted or disturbed specimen, respectively.

$$E_{0,Y_I,Intac.}^{t_{sc}} = 5.4156ln(t_{sc}) + E_{0,Y_I}^{t_{sc}=12hrs} \quad (44)$$

$$E_{0,Y_I,Recon.}^{t_{sc}} = 19.271ln(t_{sc}) + E_{0,Y_I}^{t_{sc}=12hrs} \quad (45)$$

International Journal of Engineering Research & Technology (IJERT)
ISSN: 2278-0181
Vol. 5 Issue 09, September-2016

6) Long-term consolidation effects on ELS:

$$[\varepsilon_a]^{\sigma_{ss}}_{Y_I,Int.} = \{0.0014ln(t_{sc}) - 0.0033\} + [(\varepsilon_a)_{Y_I}]^{tp}_{NC} \quad (46)$$

$$[\varepsilon_a]^{\sigma_{ss}}_{Y_I,Recon.} = \{0.0007ln(t_{sc}) - 0.0016\} + [(\varepsilon_a)_{Y_I}]^{tp}_{NC} \quad (47)$$

$[(\varepsilon_a)_{Y_I}]^{tp}_{NC}$ is the initial yield strain determined under normally consolidated conditions at a standard time period designated after the end of primary consolidation and t_{sc} is the secondary consolidation time measured in hrs. Note that $t_{sc} \geq 12hrs$.

7) Loading rate effects:

$$[\varepsilon_a]^{\dot{\varepsilon}_{SR}}_{Y_I} = 0.0014ln(\dot{\varepsilon}_{a,sr}) + 0.009 \quad (48)$$

8) Quasi-recoverability (quasi-restructuration) models

Due to the diagenetic, intricate nature and complexity of natural well cemented and highly structured clayey geomaterials, perfect recoverability is most definitely not envisaged. Nevertheless, it is considered that, with ageing, restructuration can be achieved to a certain degree. As a consequence, the restructuration models are defined predominantly as functions of secondary consolidation time. The coupling effect of strain amplitude and loading rate controlled Cyclic Prestraining (CP) has not been exhaustively examined for its inclusion at this stage.

The post-destructuration TACH Structural Recoverability Models (TACH-SRM) are mathematically defined in the following equations.

$$E_o^{SR} = \mathcal{A}^E_{SR} \ln t^{SR}_{SC} + E_o^{Pd}(t_{STC}) \quad (49)$$

The Secondary Consolidation Time (SCT) required to achieve the structural recoverability initial modulus is therefore computed from:

$$t^{SR}_{Sc}(E_o^{SR}) = exp.\left\{\frac{E_o^{SR} - E_o^{Pd}(t_{STC})}{\mathcal{A}_{SR}}\right\} \quad (50)$$

where, E_o^{SR} is the initial modulus after quasi structural recoverability, $E_o^{Pd}(t_{STC})$ is the post-destructuration initial modulus determined after Short-Term Consolidation (STC) and $\mathcal{A}^E_{SR}$=19.3 is LTC related material constant. On the other hand, the elastic yield strain is computed from,

$$[\varepsilon_a]^{SR}_{Y_I} = \mathcal{A}^E_{SR} \ln t^{SR}_{SC} + [\varepsilon_a^{Pd}(t_{STC})]_{Y_I} \quad (51)$$

Hence, the SCT required for SR is then determined as:

$$t^{SR}_{Sc}(\varepsilon_a)^{SR}_{Y_I} = exp.\left\{\frac{(\varepsilon_a)^{SR}_{Y_I} - [\varepsilon_a^{Pd}(t_{STC})]_{Y_I}}{\mathcal{A}^{\varepsilon}_{SR}}\right\} \quad (52)$$

where $(\varepsilon_a)^{SR}_{Y_I}$ is the elastic yield strain after quasi-structural recoverability, while $[\varepsilon_a^{Pd}(t_{STC})]_{Y_I}$ is that determined within STC and $\mathcal{A}^{\varepsilon}_{SR}$=7X10^{-4}. Note that in all cases, t^{SR}_{SC}=Δt^{SR}_{SC}=t^{LTC}_{SC}=t^{ST}_{SC}.

The degree of recoverability can thence be confirmed from the following relations.

$$E_o^{PR} = \mathcal{A}^E_{SR} \ln t^{SR}_{SC} + E_o^{Pd}(t_{STC}) \quad (53)$$

$$[\varepsilon_a]^{PR}_{Y_I} = \mathcal{A}^E_{SR} \ln t^{SR}_{SC} + [\varepsilon_a^{Pd}(t_{STC})]_{Y_I} \quad (54)$$

where, E_o^{PR} is the post-recovery elastic modulus, $[\varepsilon_a]^{PR}_{Y_I}$ is the post-recovery elastic yield strain and $\mathcal{A}^E_{SR}$=5.42, $\mathcal{A}^{\varepsilon}_{SR}$=1.4X10^{-3}.

9) Simulating influence of mositure – suction varation:

The influence of moisture ~ suction variation on the elastic/resilient properties can be referenced from [12].

V. Application of Proposed Models for Geomaterials Characterization

As demonstrated in the subsequent sub-Sections, the proposed TACH-QM analytical models are universally applicable for characterizing a wide range of geomaterials encountered in the field, reconstituted for in-situ improvement of subgrade and remolded for use as pavement materials.

A. Stiffness Degradation with Cumulative Progressive Loading

Fig. 14, generated from (37b), is a depiction of the impact of vibrational dynamic loading on the stiffness characteristics of varying pavement/structural subgrade layer geomaterials. The importance of precisely determining the required initial design stiffness and ultimate (permanent deformation) limit stiffness can well be appreciated.

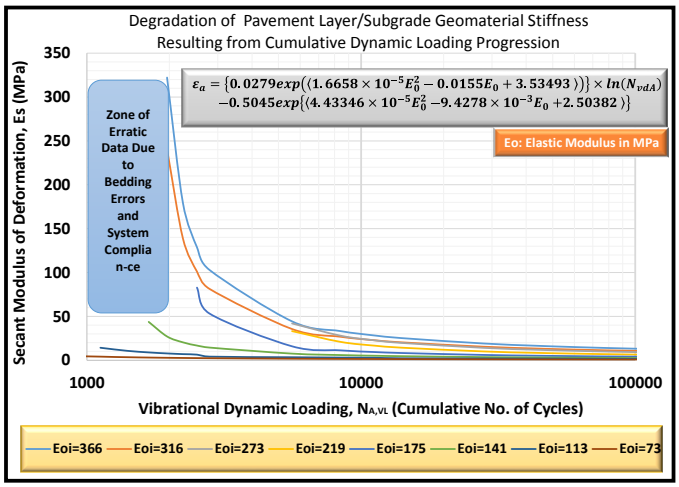

Fig. 14. Example of application of (1): Degradation of pavement/subgrade layer stiffness due to effects of progressive cumulative dynamic loading.

International Journal of Engineering Research & Technology (IJERT)
ISSN: 2278-0181
Vol. 5 Issue 09, September-2016

B. Influence of stress state and drainage conditions

1) Small strain elastic/resilient modulus: The influence of the mean effective stress on the small strain elastic/resilient modulus is demonstrated in Fig. 15 as generated from (1).

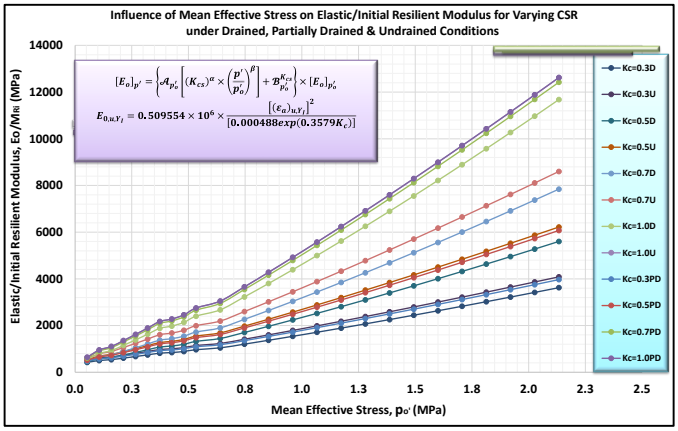

Fig. 15. Example of application of (2): Influence of mean effective stress on stiffness for varying consolidation stress ratios (CSR) and drainage conditions.

Based on the results plotted in Fig. 15, it can be noted that, notwithstanding the drainage conditions and consolidation stress history, the mean effective stress impacts the characteristics and magnitude of the elastic modulus.

2) Small strain Poisson's ratio: The characteristic curves graphically represented in Fig. 17 are generated from model equations defined in (16) ~ (22). It can mainly be inferred that: i) Poisson's Ratio (PR) is highly dependent on drainage conditions; ii) the magnitude of the PR is influenced by both the CSR and drainage conditions; and, iii) when subjected to similar drainage conditions, the PR characteristics are unique to the effects of the CSR.

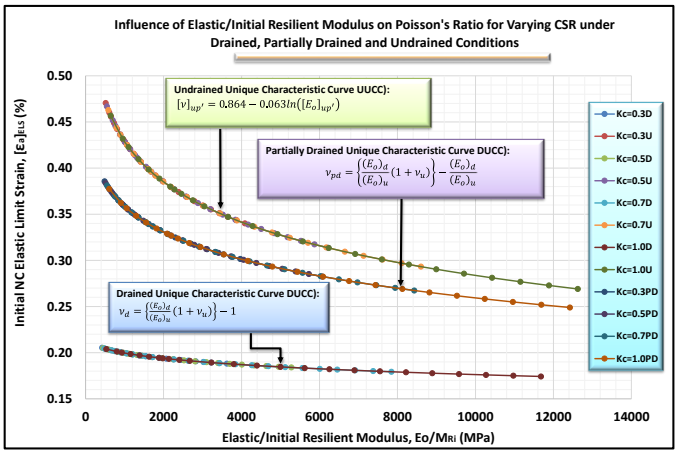

Fig. 16. Example of application of (16) ~ (22): Poisson's ratio characteristics subjected to varing drainage conditions and consolidation stress histories.

3) ElasticLimit Strain (ELS): Characteristics similar to those exhibited by the elastic modulus can be observed for the elastic limit strain depicted in Fig. 17. The curves are generated from the model equations defined in (23) ~ (32).

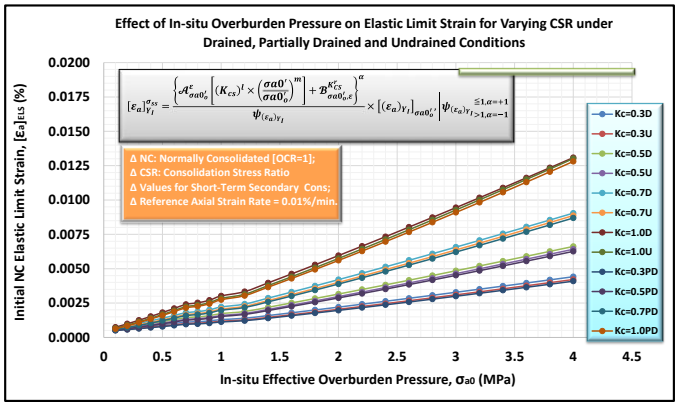

Fig. 17. Example of application of (23) ~ (32): Elastic limit strain characteristics for goematerials subjected to varying drainage conditions and consolidation stress histories defined by CSR.

4) ElasticLimit Stress (ELSt): The results plotted in Fig. 18 show the graphical correlations between the elatic modulus and the elastic limit stress simulating geomaterials subjected to varying conditions of drainage and reconsolidation stress histories. Observations, similar to those made in 2) for the Poisson's ratio, can be made from this figure.

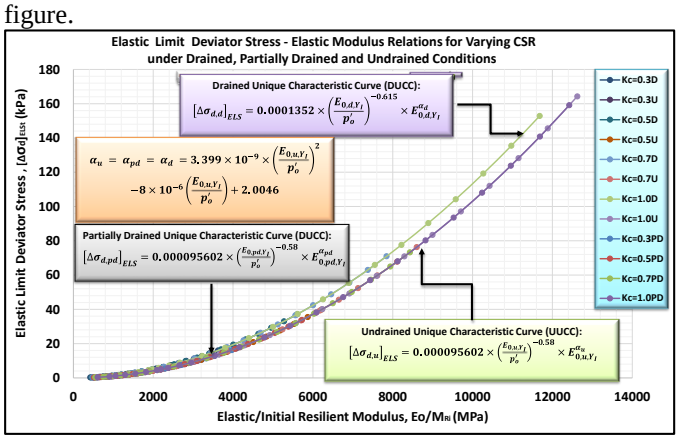

Fig. 18. Example of application of (33): Correlations between elastic modulus and elastic limit stress for varying drainage conditions and CSR.

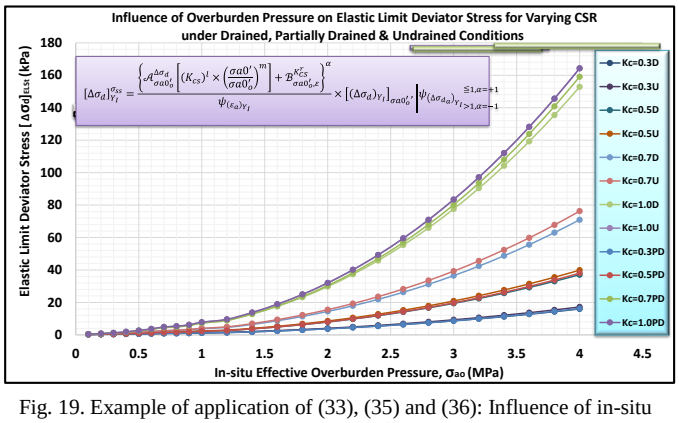

Fig. 19. Example of application of (33), (35) and (36): Influence of in-situ overburden pressure on elastic limit stress for varying consolidation stress ratios and drainage conditions.

On the other hand, observations, similar to those made in Fig. 15 for the elastic modulus can be derived for the elastic limit stress characteristics depicted in Fig. 19.

International Journal of Engineering Research & Technology (IJERT)
ISSN: 2278-0181
Vol. 5 Issue 09, September-2016

C. Influence of LTC, Strain Rate and Plasticity Index on the Stiffness Decay Characteristic Curves

The influence of Long-Term Consolidation (LTC), strain rate and Plasticity Index (PI) are reported in [18] and [19]

D. Elastic/Resilient Characteristics of Various Geomaterials

As mentioned and tabulated in the introduction, various tropical unbound and bound, unbatched and batched geomaterials were tested and characterized in this study. The materials include, but are not necessarily limited to: i) fine-grained silty clays; ii) granular lateritic gravels; iii) clacarous gravels; iv) quartzic gravels; v) limestone gravels; vi) crushed rock (stone) aggregates; geomaterials of pozzolanic nature; vii) unbound mechanically stabilized conventionally and at OBR; viii) unbound mechanically stabilized with geosynthetics; ix) OPMC stabilized; and, OPMC-GRI stabilized. Details can be perused from [12].

VI. APPLICATION OF PROPOSED MODELS FOR PB-VE DESIGNS, SPECIFICATIONS AND CONSTRUCTION QCA

Examples of recent applications of the proposed TACH-QM analytical models in the development of quasi-mechanistic performance based value engineering designs, specifications and construction QCA are provided in Figs. 20 ~ 26.

A. Design Applications

The analytical graphs depicted in Figs. 20 ~ 26 were used for generating appropriate design parameters required for the recently designed Baraawe Airport runway pavement, taxiway and aprons in Somalia, which prompted challenges due to the lack of suitable construction materials coupled with the existence of more than 4m of thick silty clayey subgrade layer.

1) Determination of appropriate Citical Replacement Depth (CRD): As depicted in Fig. 20 a new approach proposed in this Study was adopted.

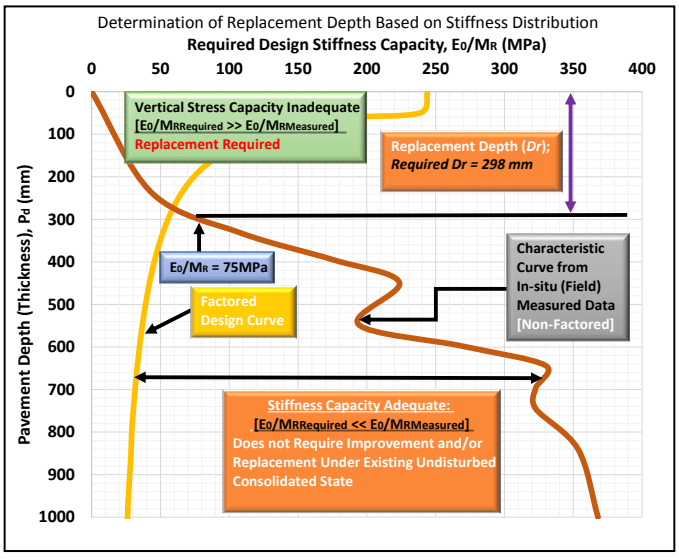

Fig. 20. Determination of Critical Replacement Depth (CRD) based on Q-M design concepts from: a) in-situ (field) stiffness measurements and, b) vertical stress distribution and in-situ dcp measurements

2) Determination of stress distribution with depth: The factored maximum vertical stress is computed from the tire pressure of the Design Aircraft by applying (55).

$$\sigma_{mvs} = 0.0113\sigma_{tp}^2 - 14.835\sigma_{tp} + 6065.2\ (kPa) \qquad (55)$$

a) Vertical stress distribution: Determined based on the maximum vertical stress value and models reported in [9].

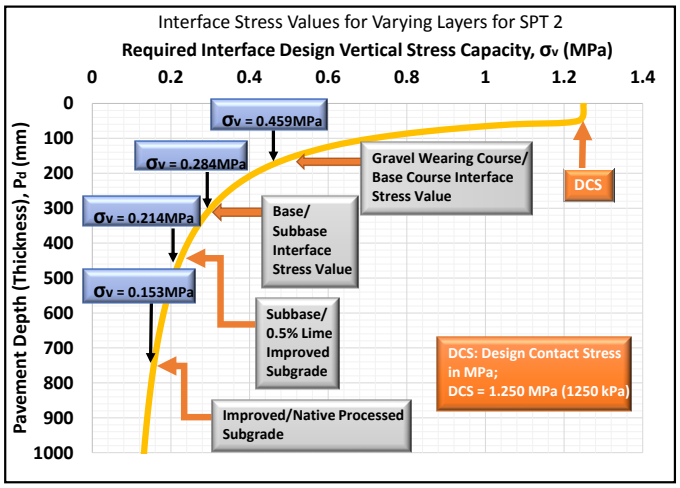

Fig. 21. Vertical stress interface values for varying pavement and subgrade layers determined based on the Q-M design concepts.

b) Lateral stress distribution: Determined based on correlation of the vertical stress multiplied with the Poisson's ratio.

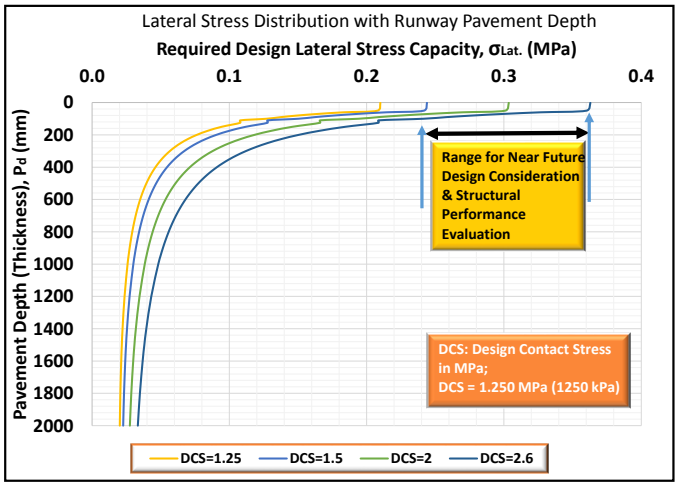

International Journal of Engineering Research & Technology (IJERT)
ISSN: 2278-0181
Vol. 5 Issue 09, September-2016

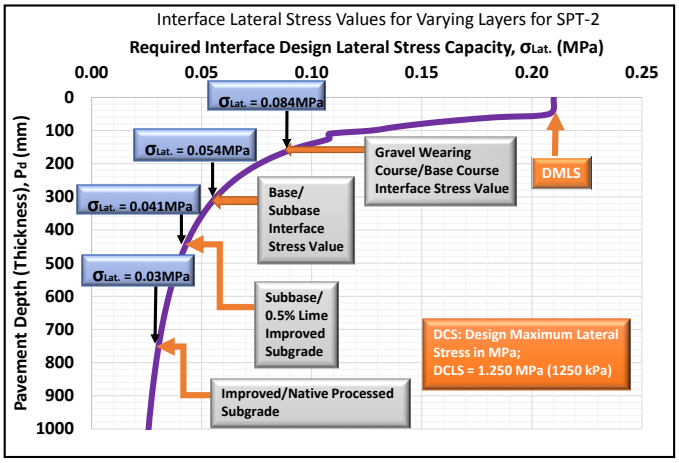

Fig. 22. Lateral stress interface values for varying pavement and subgrade layers determined based on the Q-M design concepts.

3) Determination of stiffness distribution with depth: Determined based on multi-layer elastic theory models proposed and applied in [9].

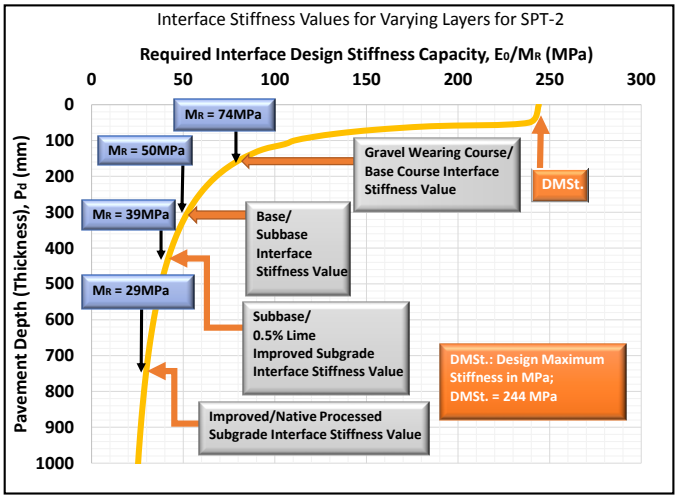

Fig. 23. Stiffness interface values for varying pavement and subgrade layers determined based on the Q-M design concepts.

4) Determination of Poisson's ratio distribution with depth: This is depicted in Fig. 24 for a wide range of vertical stresses, strains and stiffness (refer to Figs. 22, 23 and 25). Note that the interface values shown in Figures 21 ~ 26 indicate the design values required at the respective depths based on the QM analyses considering undrained conditions of the runway pavement foundation ground [10] and [15].

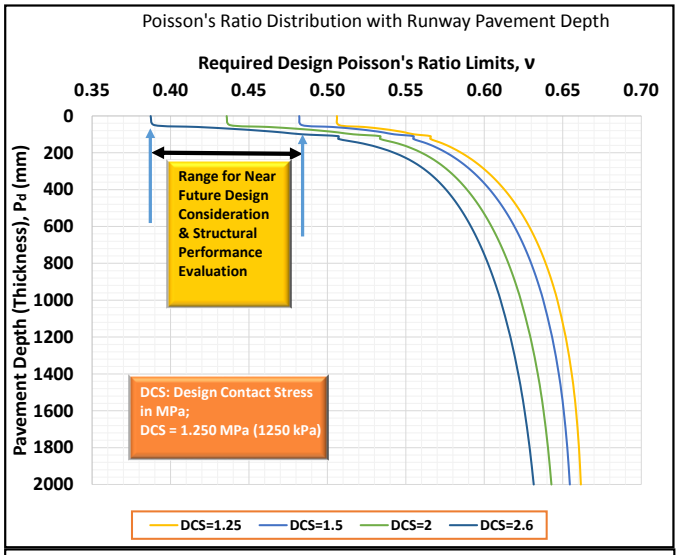

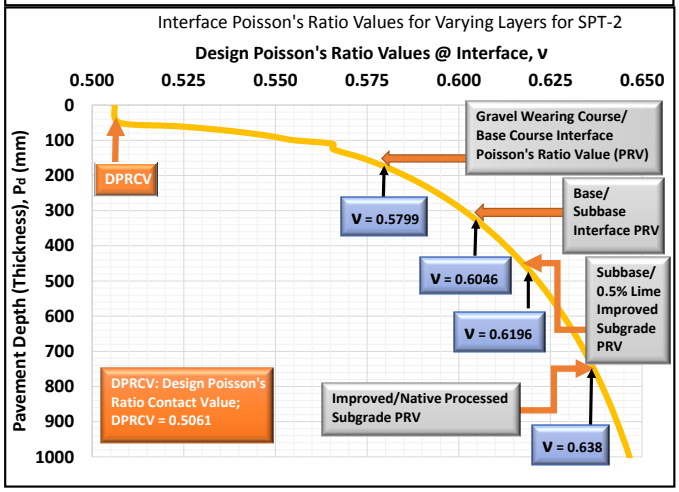

Fig. 24. Poissons's ratio interface values for varying pavement and subgrade layers determined based on the Q-M design concepts.

5) Determination of strain distribution with depth: The vertical ad lateral strain distributions are shown in Figs. 25 and 26, respectively. The lateral strains were derived from a function of the correlation with the vertical strains and Poisson's ratio. It can be derived that maximum deflections and deformation propensity are concentrated in the upper layers of the pavement gradually reducing with the increase in depth.

International Journal of Engineering Research & Technology (IJERT)
ISSN: 2278-0181
Vol. 5 Issue 09, September-2016

a) Vertical Strain: It can, however, be inferred that the vertical strains prevail within the region of small strains.

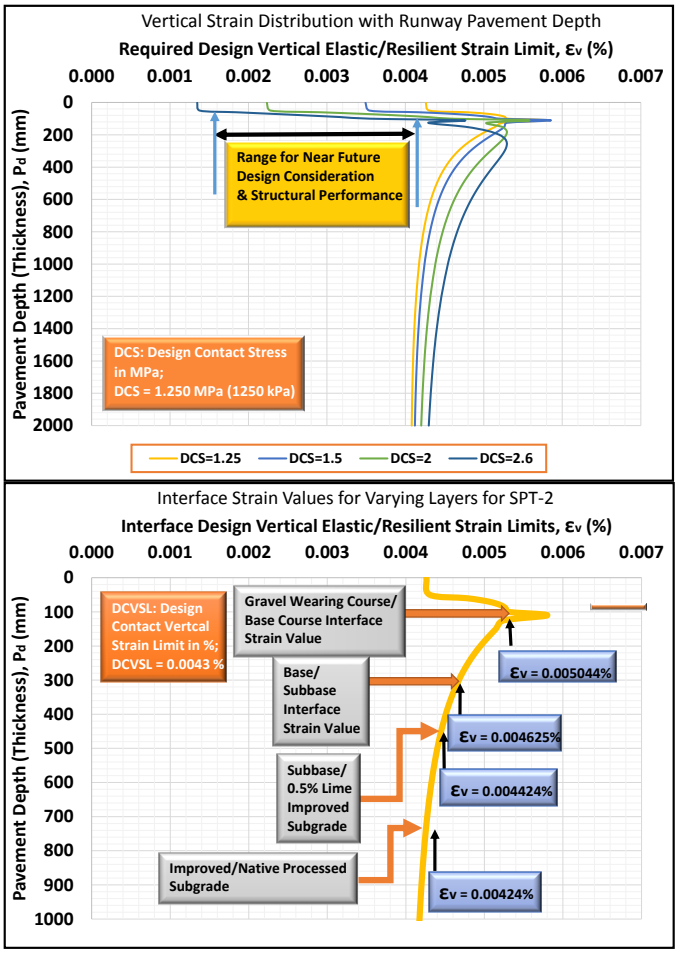

Fig. 25. Vertical strain interface values for varying pavement and subgrade layers determined based on the Q-M design concepts.

b) Lateral Strain: It can be observed that the values of the lateral strains plotted in Fig. 26 occur within the range of small strains.

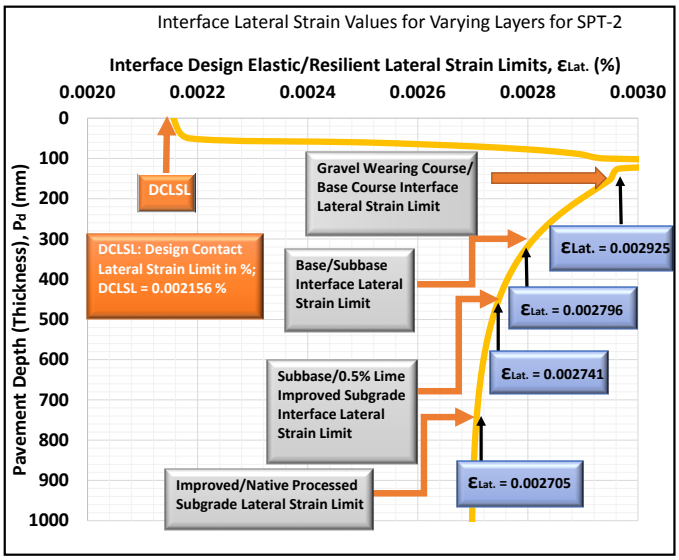

Fig. 26. Lateral strain interface values for varying pavement and subgrade layers determined based on the Q-M design concepts.

VII. Case Example of Recent Application for Airport Pavement Design

The comprehensive case example of a recent application of the TACH-MD models and Quasi-Mechanistic (Q-M) approach adopted for the design of the Baraawe Airport runway pavement in Somalia can be referenced from [10] and [15]. The pavement structural configuration of the preferred priority design is depicted in Figure 27. Note that the configuration includes a subgrade structural layer thickness that is determined based on the Q-M approach. Based on this approach sufficiently adequate PB-VE designs that culminated in construction cost-time savings of more than 40% were developed.

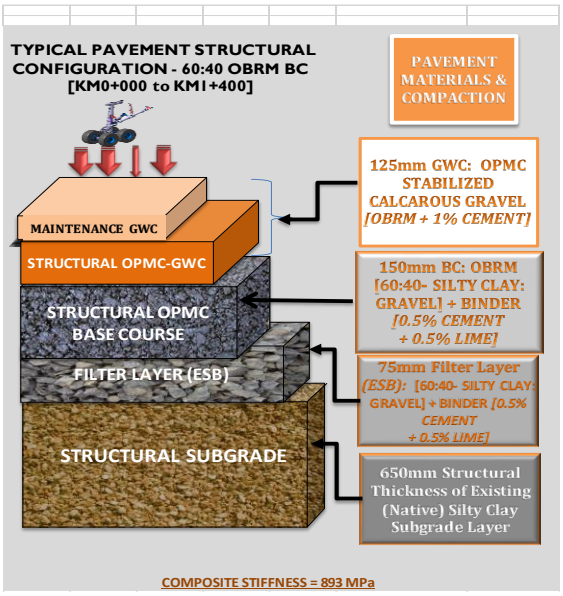

Fig. 27. Example of the priority pavement structural configuration of the Barawe Airport in Somalia developed on the basis of the TACH-QM approach employing the proposed analytical models

VIII. Conclusions

Universal and versatile analytical models equipped with a variety of application modules have been proposed in this paper. Application of the proposed models has been practically manifested through graphical examples for the characterization of geomaterials, generation of imperative design parameters and a pragmatic case example of a runway pavement structural design. The design characteristic curves and parametric values clearly indicate the validity, lucidity and rationality of the proposed analytical models and the TACH-QM method of PB-VE design for highway and airport pavements.

Acknowledgment

The Author wishes to acknowledge, with gratitude, the Materials Testing & Research Department, Ministry of Transport & Infrastructure, Kenya, as well as the Research Teams of Kensetsu Kaihatsu Engineering Consultants Limited and the Kenya Geotechnical Society (KGS). Sincere appreciation is also expressed to the Japan International Cooperation Agency (JICA), Japan Bank of International Cooperation (JBIC), Construction Project Consultants Inc., Kajima Corporation and Kajima Foundation for funding a substantial part of the study conducted in Africa.

International Journal of Engineering Research & Technology (IJERT)
ISSN: 2278-0181
Vol. 5 Issue 09, September-2016

REFERENCES

[1] AASHTO, *AASHTO Guide for Design of Pavement Structures*, American Association of State Highway and Transportation Officials, Washington, D.C., 1993.

[2] J.N. Mukabi, "Necessity for review of resilient properties and conventional resilient modulus models of characterizing pavement materials for MEPD", E-Publication in academia.edu., 2015.

[3] R.B.J. Brinkgreve and E. Engin, "Validation of geotechnical finite element analysis", Proceedings of the 18th International Conference on Soil Mechanics and Geotechnical Engineering, vol. 2, pp. 677-682, Paris 2013.

[4] J.N. Mukabi, "Characterization of consolidation stress-strain-time histories on the pre-failure behavior of natural clayey geomaterials, Proceedings of the VIth International Symosium on Deformation Characteristics on Geomaterials, Buenos Aires, 2015.

[5] J.N. Mukabi, "Innovative application of mechanical ND in-situ tests for generating pavement structural design parameters, Proceedings of the XVth Pan-American Conference on Soil Mechanics and Geotechnical Enngineering, Buenos Aires, 2015.

[6] J.N. Mukabi, "Review of DCP based CBR – UCS and resilient modulus models for application in highway and airport pavement design", Pre-print E-Publication in academia.edu.,June 2016.

[7] J.N. Mukabi, "The Proposed TACH-MDs: Revolutionary VE-PB technologies and methods of design for pavements and ancillary geo-structures", Proceedings of the World Road Congress, Seoul, November 2015.

[8] Kensetus Kaihatsu Limited, "Structural design for pavements, aprons and taxiways: Detailed Engineering Design Report No. BAP-05 for Rehabilitation and Upgrading of the Bossaso Airport Project", April, 2014.

[9] J.N. Mukabi and S.F. Wekesa, "Case examples of successful application of a new PB-VE design approach for runway pavements in East Africa", Proceedings of the World Road Congress Workshop on Airfields, Seoul, November 2015.

[10] Kensetsu Kaihatsu Consulting Engineers Limited, "Structural pavement design for pavements, aprons and taxiways: Detailed Engineering Design Report No. BAR-01DD, June, 2016.

[11] S.K. Kogi, J.N Mukabi, M. Ndeda, and S. Wekesa, "Analysis of enhanced strength and deformation resistance of some tropical geomaterials through application of in-situ based Stabilization techniques. Proceedings. 1st International Conference on Geotechniques, Environment and Materials (GEOMAT), Mie, Japan, August 2016.

[12] J.N. Mukabi, "Characterization of OBRM-OPMC-GRI stabilized geomaterials for enhanced pavement performance", unpublished.

[13] D. Mounier, "A new mechanistic design procedure for flexible airfield pavements", Conference of Airports in Urban Networks", Paris, 2014.

[14] J.N. Mukabi, "Case Study Analysis: Innovative Utilization of Sub-standard Geomaterials for Road Construction", Proceedings of the World Road Congress, Seoul, November 2015.

[15] Kensetsu Kaihatsu Consulting Engineers Limited, "Materials factial and characterization report: Report No. BAR-01GI, June, 2016.

[16] Materials Testing & Research Department, Ministry of Transport & Infrastructure, Kenya, "Studies on geosynthetics reinforced pavements and embankments", Final Detailed Engineering Report-Part I Vol.1.

[17] Materials Testing & Research Department, Ministry of Transport & Infrastructure, Kenya, "Performance evaluation of geosynthetic-reinforced earth retaining walls (RE-Walls) along Thika Highway", Final Detailed Engineering Report-Part I Vol.1.

[18] J.N. Mukabi, "Characterizing the influence of moisture-suction variation on elastic properties of tropical geomaterials", unpublished.

[19] J.N. Mukabi, "Unique attributes of moisture-suction variation on elastic limit stresses and strains of geomaterials", unpublished.

[20] J.N. Mukabi, "Expedient Elastic and Mechanical Properties of Rocks Applicable for Design, Standard Specifications and Construction QCA", Pre-print E-Publication in academia.edu., November 2015.

[21] J.N. Mukabi, "Proposed Versatile Model for Determining Poisson's ratio for civil engineering applications based on elastic modulus", Pre-print E-Publication in academia.edu., August 2015.